

CG020 Genomika

Přednáška 11

Systemová biologie

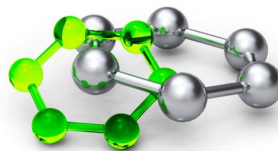
Jan Hejátko

Funkční genomika a proteomika rostlin,
Středoevropský technologický institut (CEITEC)
a

Národní centrum pro výzkum biomolekul,
Přírodovědecká fakulta,

Masarykova univerzita, Brno
hejatko@sci.muni.cz, www.ceitec.eu

MUNI
SCI



Literatura

- Literární zdroje ke kapitole 11:

- Wilt, F.H., and Hake, S. (2004). *Principles of Developmental Biology*. (New York ; London: W. W. Norton)
- Eden, E., Navon, R., Steinfeld, I., Lipson, D., and Yakhini, Z. (2009). GOrilla: a tool for discovery and visualization of enriched GO terms in ranked gene lists. *BMC Bioinformatics* 10, 48.
- The Arabidopsis Genome Initiative. (2000). Analysis of the genome sequence of the flowering plant *Arabidopsis thaliana*. *Nature* 408, 796-815.
- Benitez, M. and Hejatko, J. Dynamics of cell-fate determination and patterning in the vascular bundles of *Arabidopsis thaliana* (submitted)
- de Luis Balaguer MA, Fisher AP, Clark NM, Fernandez-Espinosa MG, Moller BK, Weijers D, Lohmann JU, Williams C, Lorenzo O, Sozzani R. 2017. Predicting gene regulatory networks by combining spatial and temporal gene expression data in *Arabidopsis* root stem cells. *Proc Natl Acad Sci U S A* 114(36): E7632-E7640.

Osnova

- Definice **Systemové biologie**
- **Nástroje**
 - **Genová ontologie**
 - **Bayesovské sítě**
 - **Modelování molekulárních/genových regulačních sítí**
 - **Odvození genových regulačních sítí z velkých omických datových sad**

Definice

Systémová biologie je vědecký směr v biologii využívající přístupy dalších věd, především **biochemie, chemie, informatiky a matematiky**. Zabývá se **studiem biologických funkcí a mechanismů** vzniklých následkem **komplexních interakcí** v biologických systémech.

Základní myšlenkou je **komplexní pohled**, opak **redukcionismu** (který je převládajícím paradigmatem například v molekulární biologii), tedy předpoklad, že **systém je víc než součet jeho částí**.

Systémová biologie často **pracuje s modely**, které jsou vytvářeny **matematickými a informatickými přístupy** na **základě biologických dat**, jejichž vlastnosti jsou posléze porovnávány s vlastnostmi živých systémů (**Wikipedia**).

Definice

Systemová biologie se zabývá studiem biologických systémů, jejichž chování nelze redukovat na *lineární součet funkcí jejich částí*. Systemová biologie nemusí nutně zahrnovat velké množství komponent nebo rozsáhlých datových souborů, jako je tomu v genomice nebo konektomice, ale často vyžaduje metody kvantitativního modelování vypůjčené z fyziky (Nature).

Definice

Názorně vysvětluje video Dr. Nathana Price,
zástupce ředitele Ústavu pro systémovou biologii, Seattle, USA na
https://www.youtube.com/watch?v=OrXRI_8UFHU.



Osnova

- Definition of Systems Biology
- Tools
 - Gene Ontology analysis

Výsledky –omických studií vs. biologicky relevantní závěry

- Výsledky –omických studií reprezentují **enormní množství dat**, např. geny s rozdílnou expresí. Ale jak z nich získat **biologicky relevantní závěry**?

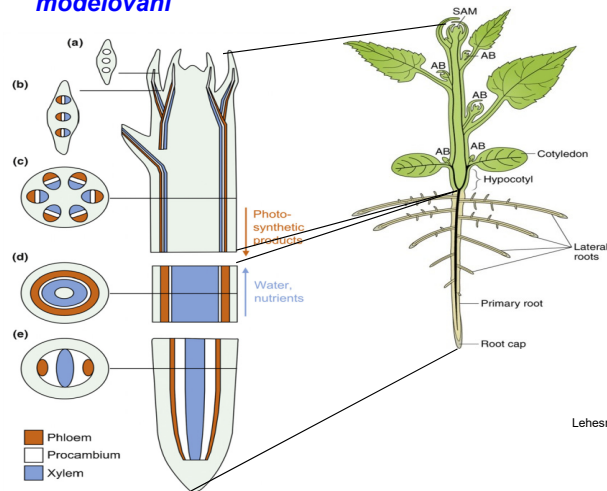
Ddii et al., unpublished

gene	locus	sample_1	sample_2	status	value_1	value_2	log2(fold_change)	test_stat	p_value	q_value	significant
AT1G07795	1:2414285-2414967	WT	MT	OK	0	1.1804 1.79769e+308		1.79769e+308	6.88885e-05	0.00039180	1 yes
HRS1	1:4556891-4558708	WT	MT	OK	0	0.696583 1.79769e+308		1.79769e+308	6.61994e-08	4.67708e-05	yes
ATML014	1:9227472-9232296	WT	MT	OK	0	0.514609 1.79769e+308		1.79769e+308	9.74219e-05	0.00053505	5 yes
NRT1.6	1:9400663-9403789	WT	MT	OK	0	0.877865 1.79769e+308		1.79769e+308	3.2692e-08	3.50131e-07	yes
AT1G27570	1:9575425-9582376	WT	MT	OK	0	2.0829 1.79769e+308		1.79769e+308	9.76039e-06	6.647e-05	yes
AT1G60095	1:22159735-22162419	WT	MT	OK	0	0.688588 1.79769e+308		1.79769e+308	9.94952e-08	9.95901e-08	yes
AT1G03020	1:698206-698515	WT	MT	OK	0	1.78859 1.79769e+308		1.79769e+308	0.00913915	0.0277958	yes
AT1G13609	1:4662720-4663471	WT	MT	OK	0	3.55814 1.79769e+308		1.79769e+308	0.00021683	0.00108079	yes
AT1G21550	1:7553100-7553876	WT	MT	OK	0	0.562868 1.79769e+308		1.79769e+308	0.00115582	0.00471497	yes
AT1G22120	1:7806308-7808632	WT	MT	OK	0	0.617354 1.79769e+308		1.79769e+308	2.48392e-06	0.00028514	yes
AT1G31370	1:11238297-11239363	WT	MT	OK	0	1.46254 1.79769e+308		1.79769e+308	4.83523e-05	0.00028514	3 yes
APUM10	1:13283397-13285570	WT	MT	OK	0	0.581031 1.79769e+308		1.79769e+308	7.87855e-06	5.46603e-05	yes
AT1G48700	1:18010728-18012871	WT	MT	OK	0	0.556525 1.79769e+308		1.79769e+308	6.53917e-05	0.00037473	6 yes
AT1G59077	1:21746209-21833195	WT	MT	OK	0	138.886 1.79769e+308		1.79769e+308	0.00122789	0.00496816	yes
AT1G60050	1:22121549-22123702	WT	MT	OK	0	0.370087 1.79769e+308		1.79769e+308	0.00117953	0.0048001	yes
AT4G15242	4:8705786-8706997	WT	MT	OK	0.00930712	17.9056	10.9098	-4.40523	1.05673e-05	7.13983e-05	yes
ATS33251	5:12499071-12500433	WT	MT	OK	0.0498375	52.2837	10.0349	-9.8119	0	0	0 yes
AT4G12520	4:7421055-7421738	WT	MT	OK	0.0195111	15.8516	9.66612	-3.90043	9.60217e-05	0.000528904	yes
AT1G60020	1:22100651-22105276	WT	MT	OK	0.0118377	7.18823	9.24611	-7.50382	6.19504e-14	1.4988e-12	yes
ATS315360	5:4987235-4989182	WT	MT	OK	0.0988273	56.4834	9.1587	-10.4392	0	0	0 yes

Example of an output of transcriptional profiling study using Illumina sequencing performed in our lab. Shown is just a tiny fragment of the complete list, comprising about 7K genes revealing differential expression in the studied mutant.

Vývoj rostlinných vodivých pletiv

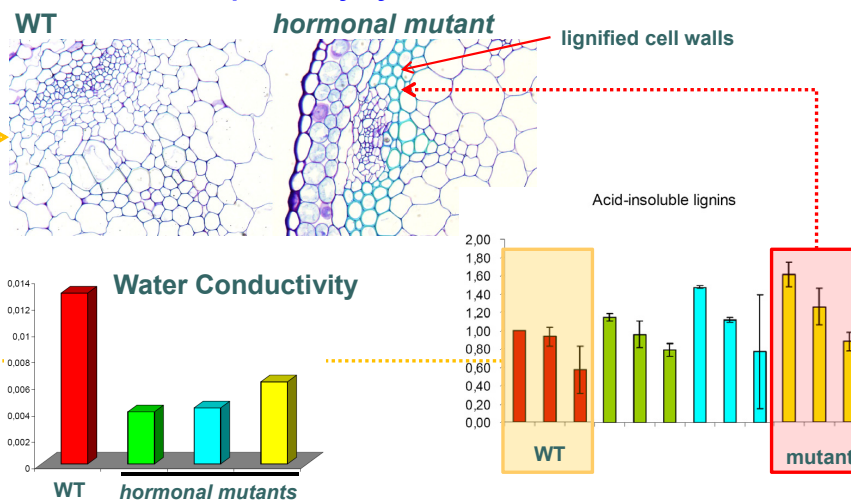
- **Vodivé pletivo** jako vývojový model pro **GO analýzu** a **MRN modelování**



Lehesranta et al., *Trends in Plant Sci* (2010)

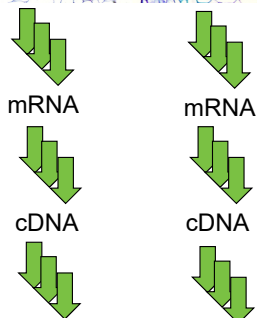
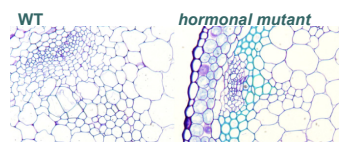
Hormonální regulace vývoje rostlinných vodivých pletiv

- Rostlinné hormony regulují ukládání ligninu v buněčných stěnách a transport vody xylemem



Hormonální regulace vývoje rostlinných vodivých pletiv

- **Transkripční profilování** pomocí **sekvenování RNA**



Sekvenování společností Illumina a určení počtu transkriptů

Výsledky – omických studií vs. biologicky relevantní závěry

- Transkripční profilování identifikovalo víc než **9K odlišně regulovaných genů...**

Ddii et al., unpublished

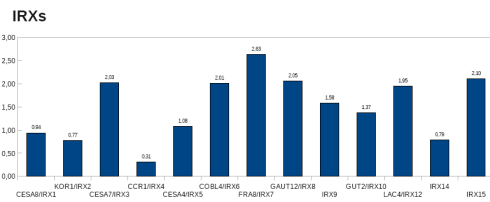
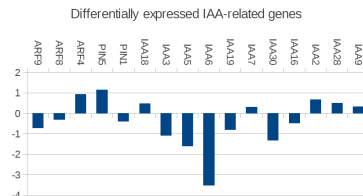
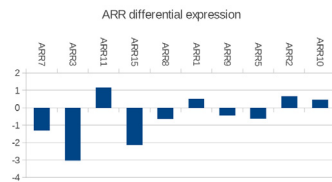
gene	locus	sample_1	sample_2	status	value_1	value_2	log2(fold_change)	test_stat	p_value	q_value	significant
AT1G07795	1:2414285-2414967	WT	MT	OK	0	1.1804 1.79769e+308		1.79769e+308	6.88885e-05	0.00039180	1 yes
HRS1	1:4556891-4558708	WT	MT	OK	0	0.696583 1.79769e+308		1.79769e+308	6.61994e-06	4.67708e-05	yes
ATML014	1:9227472-9232296	WT	MT	OK	0	0.514609 1.79769e+308		1.79769e+308	9.74219e-05	0.00053505	5 yes
NRT1.6	1:9400663-9403789	WT	MT	OK	0	0.877865 1.79769e+308		1.79769e+308	3.2692e-08	3.50131e-07	yes
AT1G27570	1:9575425-9582376	WT	MT	OK	0	2.0829 1.79769e+308		1.79769e+308	9.76039e-06	6.647e-05	yes
AT1G60095	1:22159735-22162419	WT	MT	OK	0	0.688588 1.79769e+308		1.79769e+308	9.94932e-08	9.95901e-08	yes
AT1G03020	1:698206-698515	WT	MT	OK	0	1.78859 1.79769e+308		1.79769e+308	0.00913915	0.0277958	yes
AT1G13609	1:4662720-4663471	WT	MT	OK	0	3.55814 1.79769e+308		1.79769e+308	0.00021683	0.00108079	yes
AT1G21550	1:7553100-7553876	WT	MT	OK	0	0.562868 1.79769e+308		1.79769e+308	0.00115582	0.00471497	yes
AT1G22120	1:7806308-7806632	WT	MT	OK	0	0.617354 1.79769e+308		1.79769e+308	2.48392e-06	0.00028514	yes
AT1G31370	1:11238297-11239363	WT	MT	OK	0	1.46254 1.79769e+308		1.79769e+308	4.83523e-05	3	yes
APUM10	1:13253397-13255570	WT	MT	OK	0	0.581031 1.79769e+308		1.79769e+308	7.87855e-06	5.46603e-05	yes
AT1G48700	1:18010728-18012871	WT	MT	OK	0	0.556525 1.79769e+308		1.79769e+308	6.53917e-05	0.00037473	6 yes
AT1G59077	1:21746209-21833195	WT	MT	OK	0	138.886 1.79769e+308		1.79769e+308	0.00122789	0.00496816	yes
AT1G60050	1:22121549-22123702	WT	MT	OK	0	0.370087 1.79769e+308		1.79769e+308	0.00117953	0.0048001	yes
AT4G15242	4:8705786-8706997	WT	MT	OK	0.00930712	17.9056	10.9098	-4.40523	1.05673e-05	7.13983e-05	yes
ATS33251	5:12499071-12500433	WT	MT	OK	0.0498375	52.2837	10.0349	-9.8119	0	0	yes
AT4G12520	4:7421055-7421738	WT	MT	OK	0.0195111	15.8516	9.66612	-3.90043	9.60217e-05	0.000528904	yes
AT1G60020	1:22100651-22105276	WT	MT	OK	0.0118377	7.18823	9.24611	-7.50382	6.19504e-14	1.4989e-12	yes
ATS315360	5:4987235-4989182	WT	MT	OK	0.0988273	56.4834	9.1587	-10.4392	0	0	yes

12

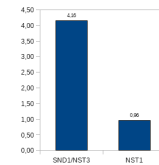
Example of an output of transcriptional profiling study using Illumina sequencing performed in our lab. Shown is just a tiny fragment of the complete list, comprising about 7K genes revealing differential expression in the studied mutant.

Genová ontologie

- Jedním z možných přístupů je studium **genové ontologie**, tj. dříve prokázané **spojitosti** mezi geny a **biologickými procesy**



XYLEM MARKERS



Genová ontologie

- Několik nástrojů umožňuje **statisticky vyhodnotit obohacení** o geny **spojené se specifickými procesy**

Eden et al., *BMC Bioinformatics* (2009)

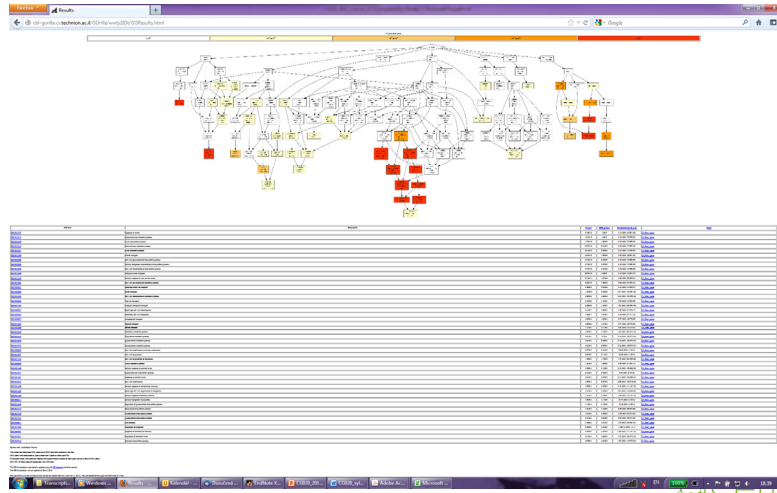
The screenshot shows the GORILLA web interface. At the top, it says "GORILLA Gene Ontology enrichment analysis and visualization tool". Below this, there is a small graphic of a gorilla and a heatmap. The main content area contains instructions for using the tool, including a list of steps: "Step 1: Choose organism", "Step 2: Choose ranking method", "Step 3: Paste a ranked list of gene names", and "Step 4: Choose an ontology". There are also links for "Browse example", "User instructions", "GORILLA News", "Submit Feedback", and "References". At the bottom, there is a search bar with the text "Search Enriched GO terms" and a "Submit form" button. The browser's address bar shows "http://cbl-gorilla.cs.technion.ac.il".

14

One of such recent and very useful tools is Gorilla software, freely available at <http://cbl-gorilla.cs.technion.ac.il/>.

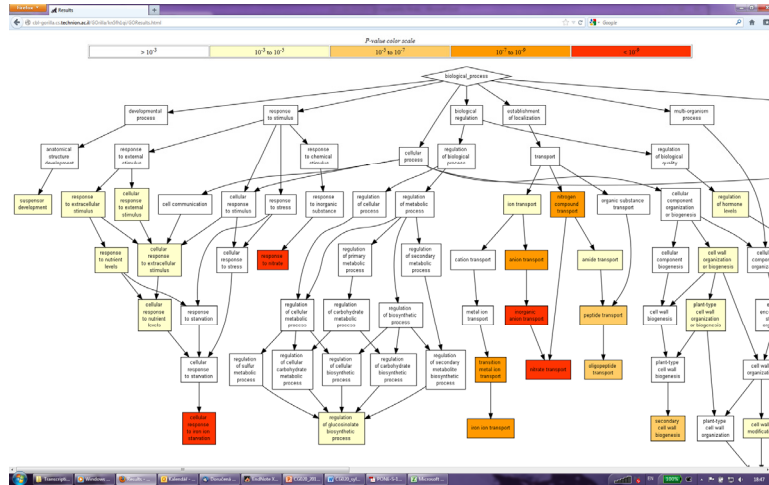
Genová ontologie

- Několik nástrojů umožňuje **statisticky vyhodnotit obohacení** o geny **spojené se specifickými procesy**



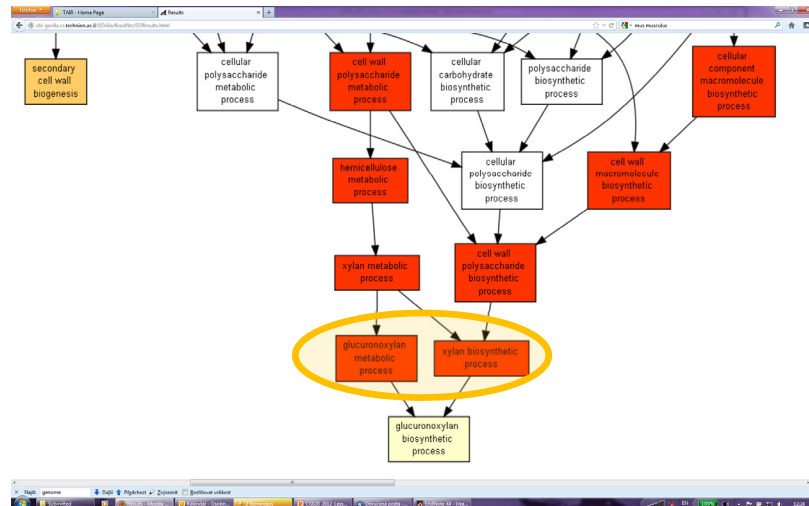
Genová ontologie

- Několik nástrojů umožňuje **statisticky vyhodnotit obohacení** o geny **spojené se specifickými procesy**



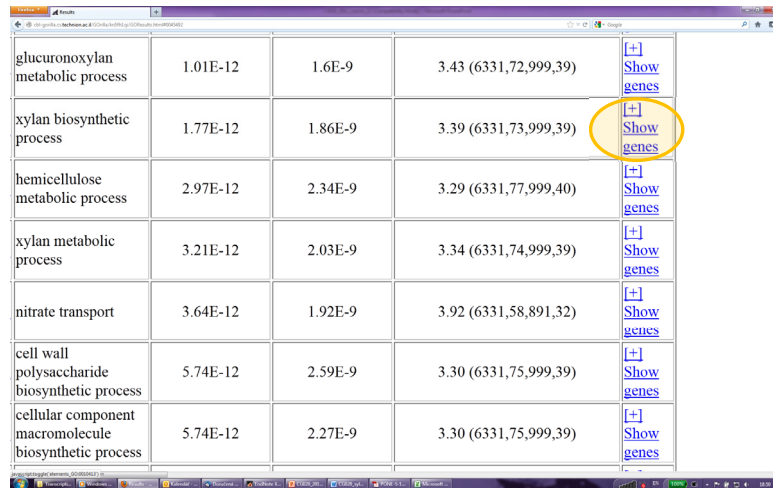
Genová ontologie

- Několik nástrojů umožňuje **statisticky vyhodnotit obohacení** o geny **spojené se specifickými procesy**



Genová ontologie

- Několik nástrojů umožňuje **statisticky vyhodnotit obohacení** o geny **spojené se specifickými procesy**



glucuronoxylan metabolic process	1.01E-12	1.6E-9	3.43 (6331,72,999,39)	[+] Show genes
xylan biosynthetic process	1.77E-12	1.86E-9	3.39 (6331,73,999,39)	[+] Show genes
hemicellulose metabolic process	2.97E-12	2.34E-9	3.29 (6331,77,999,40)	[+] Show genes
xylan metabolic process	3.21E-12	2.03E-9	3.34 (6331,74,999,39)	[+] Show genes
nitrate transport	3.64E-12	1.92E-9	3.92 (6331,58,891,32)	[+] Show genes
cell wall polysaccharide biosynthetic process	5.74E-12	2.59E-9	3.30 (6331,75,999,39)	[+] Show genes
cellular component macromolecule biosynthetic process	5.74E-12	2.27E-9	3.30 (6331,75,999,39)	[+] Show genes

Genová ontologie

- Několik nástrojů umožňuje **statisticky vyhodnotit obohacení** o geny **spojené se specifickými procesy**

Description	P-value	FDR q-value	Enrichment (N, B, n, b)	Genes
response to nitrate	4.76E-13	1.5E-9	4.13 (6331,55,891,32)	[+] Show genes
glucuronoxylan metabolic process	1.01E-12	1.6E-9	3.43 (6331,72,999,39)	[+] Show genes
xylan biosynthetic process	1.77E-12	1.86E-9	3.39 (6331,73,999,39)	[+] Hide genes SUPT7 - putative glycosyltransferase PQR93 - plant glycoamin-like starch synthase protein 3 PRAJ - enolase-like protein GAUT13 - alpha 1,4 galactanoseyltransferase JATG02490 - bifunctional salivary lipid-transfer protein/seed storage 2a albumin-like protein JATG41106 - pectinase 6a JATG10910 - rmg-h2 finger protein atf72 LACT7 - lactase 17 KNAT7 - knox-box protein knotted 1 like 7 NAC12 - nac domain containing protein 12 EXX - exon like protein 4 JATG70590 - pectin lyase-like protein KSA4 - cellulose synthase catalytic subunit 4 [udp-forming] JATG08840 - rho gpiase activating protein with pak-box p21-like-binding domain CIL2 - cellulase like protein 2 EXX - exon like protein 4 MYB63 - myb domain protein 63 PGE91 - plant glycoamin-like starch synthase protein 1 JATG46140 - putative o-acetyltransferase JATG21170 - hypothetical protein JATG70200 - agmatyl proteinase-like protein JATG09440 - protein kinase family protein JATG49020 - pathogenesis-related thionin-like protein JATG24990 - integrin protein for ncp2-like protein JATG47110 - hypothetical protein JATG16210 - bcl-2-like domain-containing protein JATG18190 - hypothetical protein P490 - putative polygalacturonase pectinase catalytic subunit p490 MAP70 - intracellular-associated protein 70-9 JATG40230 - hypothetical protein JALM4 - protein, agmatase-like 4a EXX12 - exon-like 4 NAC173 - nac domain containing protein 73 EXX - exon like protein 4 JATG27420 - hypothetical protein MYB6 - myb domain protein myb6 JATG72220 - rmg-h2 finger protein atf24 TRD1 - rnae efflux family protein JATG13800 - hypothetical protein

Osnova

- Definice Systémové biologie
- Nástroje
 - Genová ontologie
 - Bayesovské sítě

Bayesovské sítě

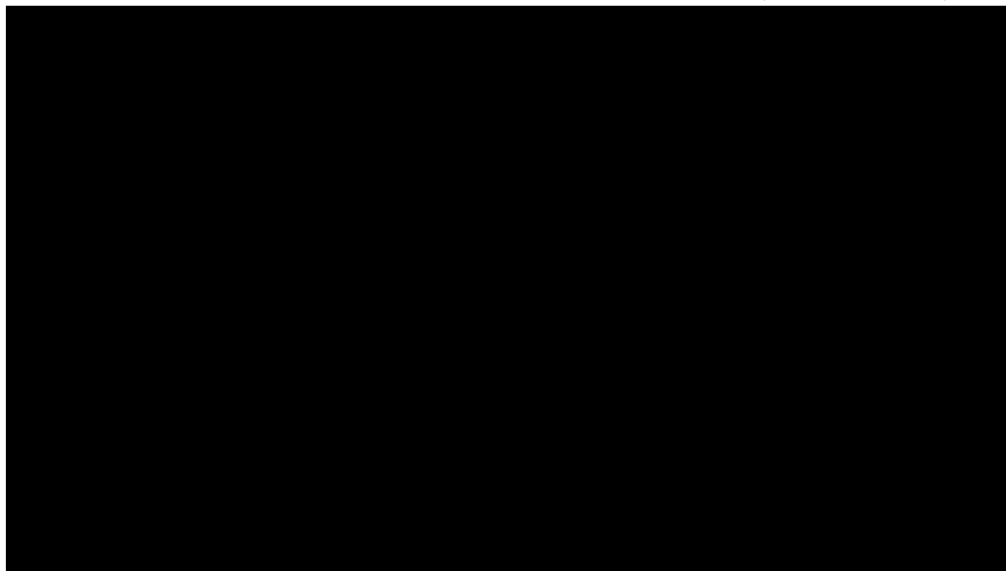
Co je Bayesovská síť?

- **Pravděpodobný grafický model**, který se používá k **vytváření modelů z dat a/nebo názoru odborníka**



Bayesovské sítě

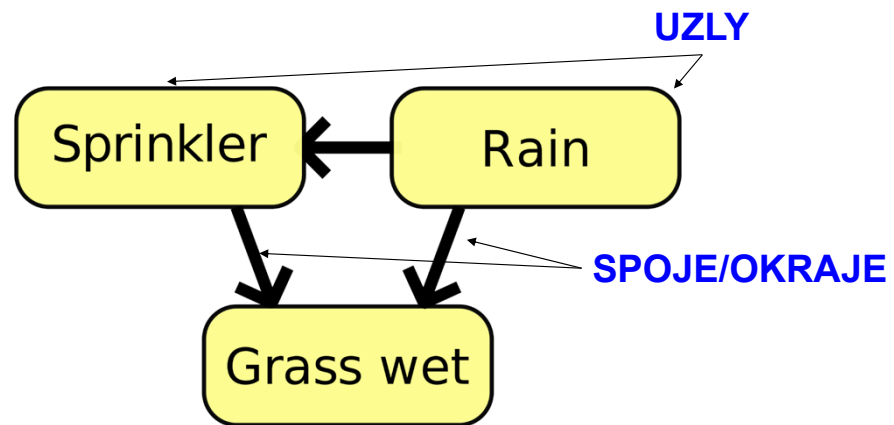
<https://www.youtube.com/watch?v=4fcqzVJwHM>



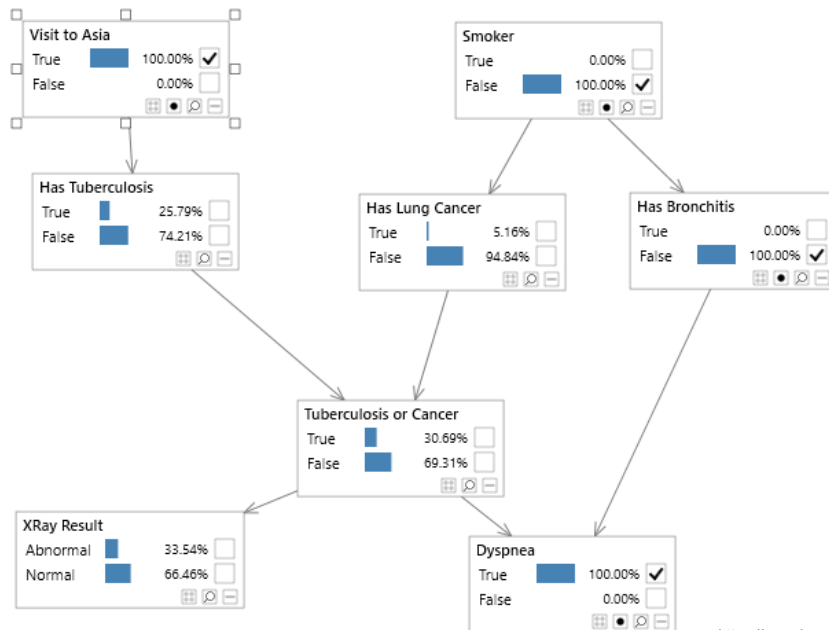
Bayesovské sítě

- Co je **Bayesovská síť**?
 - Pravidelný grafický model, který se používá k vytváření modelů z dat a/nebo názoru odborníka
 - může být využit v široké škále úkolů včetně **predikce, detekce anomálie, diagnostiky, automatického pohledu na věc, uvažování, predikce časové řady a rozhodování za nejistoty**
- **UZLY**
 - každý uzel představuje **proměnnou**, jako je výška, věk nebo pohlaví. Proměnná může být **diskrétní**, jako například pohlaví = {samičí, samčí}, nebo **spojitá**, jako např. věk
- **SPOJE**
 - přidány **mezi uzly**, aby ukazovaly, že **jeden uzel má přímý vliv na druhý**

Bayesovské sítě



Asijská Bayesovská síť



25

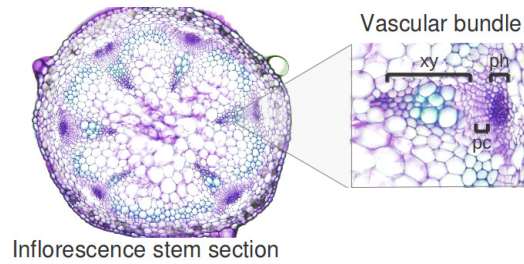
<https://www.bayesserver.com/> **CEITEC**

Osnova

- Definice Systémové biologie
- Nástroje
 - Genová ontologie
 - Bayesovské sítě
 - Modelování molekulárních/genových regulačních sítí

Modelování molekulárních regulačních sítí

- **Vodivé pletivo** jako vývojový model pro **MRN modelování**



Benítez and Hejatko, *PLoS One*, 2013

Modelování molekulárních regulačních sítí

□ Vyhledávání publikovaných dat a vytvoření malé databáze

Interaction	Evidence	References
A-ARRs – CK signaling	Double and higher order type-A ARR mutants show increased sensitivity to CK.	[27]
	Spatial patterns of A-type ARR gene expression and CK response are consistent with partially redundant function of these genes in CK signaling.	[27]
	A-type ARR decreases B-type ARR6-LUC.	[13]
	Note: In certain contexts, however, some A-ARRs appear to have effects antagonistic to other A-ARRs.	[27]
AHP6 – AHP	ahp6 partially recovers the mutant phenotype of the CK receptor WOL.	[9]
	Using an in vitro phosphotransfer system, it was shown that, unlike the AHPs, native AHP6 was unable to accept a phosphoryl group. Nevertheless, AHP6 is able to inhibit phosphotransfer from other AHPs to ARR6.	[9]

Benitez and Hejatko, PLoS One, 2011

CEITEC

Modelování molekulárních regulačních sítí

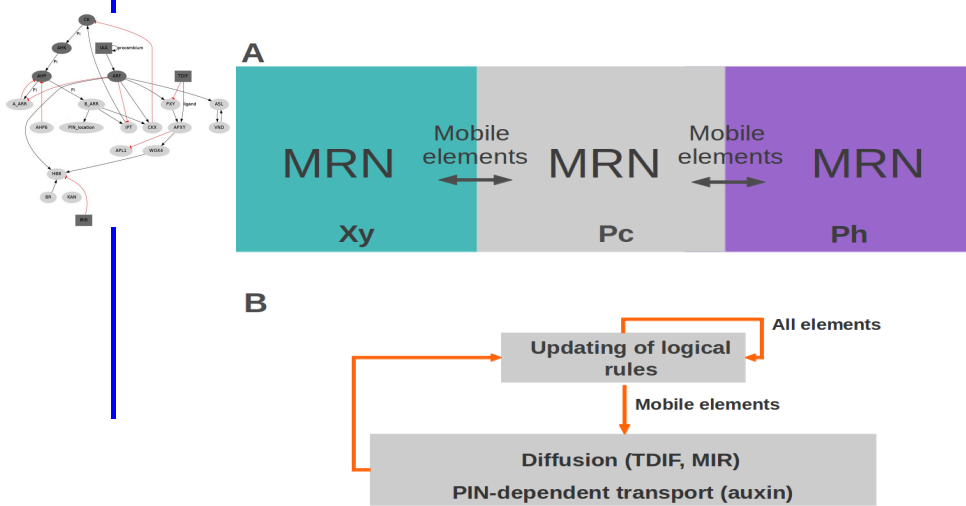
- Formulace *logických pravidel* definujících *dynamiku modelu*

Network node	Dynamical rule
CK	2 If ipt=1 and cxx=0 1 If ipt=1 and cxx=1 0 else
CKX	1 If barr>0 or arf=2 0 else
AHKs	ahk=ck
AHPs	2 If ahk=2 and ahp6=0 and aarr=0 1 If ahk=2 and (ahp6+aarr<2) 1 If ahk=1 and ahp6<1 0 else
B-Type ARRs	1 If ahp>0 0 else
A-Type ARRs	1 If arf<2 and ahp>0 0 else

Benítez and Hejatko, *PLoS One*, 2013

Modelování molekulárních regulačních sítí

- Specifikace **mobilních prvků** a jejich chování v modelu



30

GENEC

According to experimental evidence for the system under study, the hormone IAA, the peptide TDIF, and the microRNA MIR165/6 are able to move among the cells. In the case of TDIF and MIR165/6, the mobility is defined as diffusion and is given by the following equation:

$$g(t+1)T[i] = H(g(t)[i] + D(g(t)[i+1] + g(t)[i-1] - N(g(t)[i]) - b)) \quad (2),$$

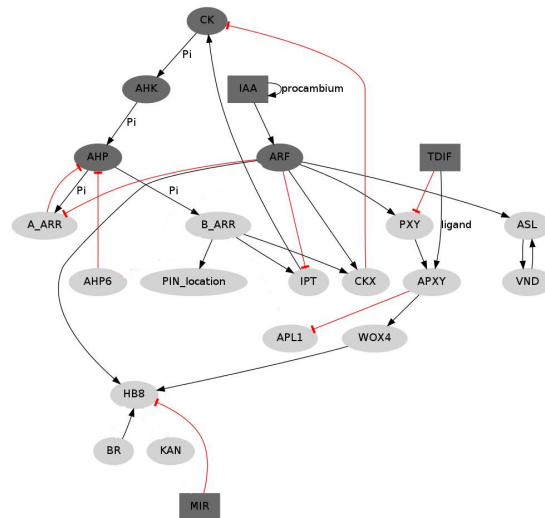
where $g(t)T[i]$ is the total amount of TDIF or MIR165 in cell (i). D is a parameter that determines the proportion of g that can move from any cell to neighboring ones and is correlated to the diffusion rate of g . b is a constant corresponding to a degradation term. H is a step function that converts the continuous values of g into a discrete variable that may attain values of 0, 1 or 2. N stands for the number of neighbors in each cell. Boundary conditions are zero-flux. In the case of IAA, the mobility is defined as active transport dependent on the radial localization of the PIN efflux transporters and is defined by the equation:

$$iaa(t+1)T[i] = H(iaa(t)[i] + Diaa(pin(t)[i+1])(iaa(t)[i+1]) + Diaa(pin(t)[i-1])(iaa(t)[i-1]) - N(Diaa)(pin(t)[i])(iaa(t)[i]) - b) \quad (3),$$

where $Diaa$ is a parameter that determines the proportion of IAA that can be transported among cells. The transport depends on the presence of IAA and PIN in the cells and b corresponds to a degradation term. As in equation 2, H is a step function that converts the continuous values to discrete ones and N stands for the number of neighbors in each cell. Boundary conditions for IAA motion are also zero-flux.

Modelování molekulárních regulačních sítí

- Příprava *první verze* modelu a její *testování*



31

CEITEC

The proposed model considers data that we identified and evaluated through an extensive search (up to January 2012). It takes into account molecular interactions, hormonal and expression patterns, and cell-to-cell communication processes that have been reported to affect vascular patterning in the bundles of Arabidopsis. The model components and interactions are graphically presented in the figure above. In the network model, nodes stand for molecular elements regulating one another's activities. Most of the nodes can take only 1 or 0 values (light gray nodes in the figure), corresponding to "present" or "not present," respectively. Since the formation of gradients of hormones and diffusible elements may have important consequences in pattern formation, mobile elements TDIF and MIR, as well as members of the CK and IAA signaling systems, can take 0, 1 or 2 values (dark gray nodes in the figure above) Benitez and Hejatko, PLoS One, 2013.

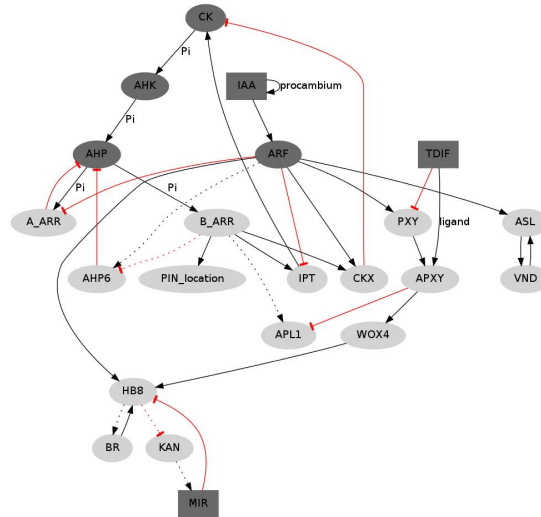
Modelování molekulárních regulačních sítí

□ Specifikace chybějících interakcí ze *známých predikcí*

Interaction	Evidence	References
CK → PIN7 radial localization	Predicted interaction (could be direct or indirect)	
	Informed by the following data: During the specification of root vascular cells in <i>Arabidopsis thaliana</i> , CK regulates the radial localization of PIN7.	[18]
	Expression of PIN7::GFP and PIN7::GUS is upregulated by CK with no significant influence of ethylene.	[18,20]
CK → APL	Predicted interaction (could be direct or indirect)	
	Consistent with the fact that APL overexpression prevents or delays xylem cell differentiation, as does CKs.	[21]
	Partially supported by microarray data and phloem-specific expression patterns of CK response factors.	(TAIR, ExpressionSet: 1005823559, [22])

Modelování molekulárních regulačních sítí

- Příprava **další verze** modelu a její **testování**



Benítez and Hejatko, *PLoS One*, 2013

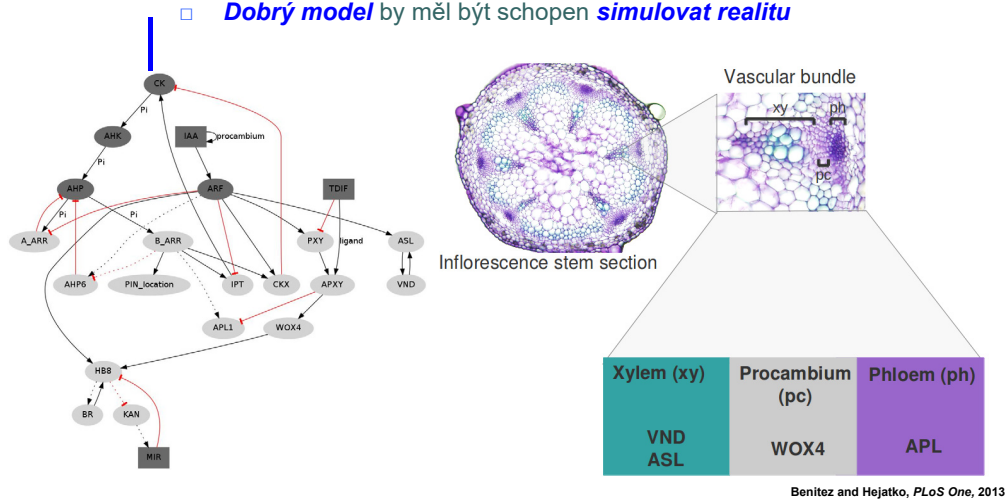
33

CEITEC

In comparison to the model shown on slide 21, the final version of the model contains the predicted interactions (dashed lines).

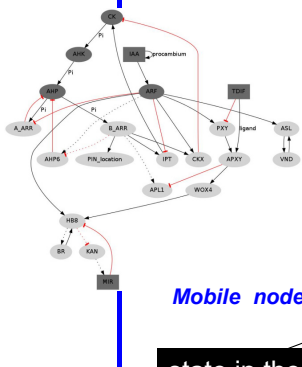
Modelování molekulárních regulačních sítí

□ **Dobrý model** by měl být schopen **simulovat realitu**



Modelování molekulárních regulačních sítí

- Formulace *rovníc* popisujících *vzájemné vztahy* v modelu



logical rule function state in the time t

Static nodes: $g_n(t+1) = F_n(g_{n1}(t), g_{n2}(t), \dots, g_{nk}(t))$

state in the time $t+1$

Amount of TDIF or MIR165 in cell i

Mobile nodes: $g_{(t+1)\tau [i]} = H(g_{(t) [i]} + D (g_{(t) [i+1]} + g_{(t) [i-1]} - N(g_{(t) [i]}) - b)$

state in the time $t+1$

constant corresponding to a degradation term

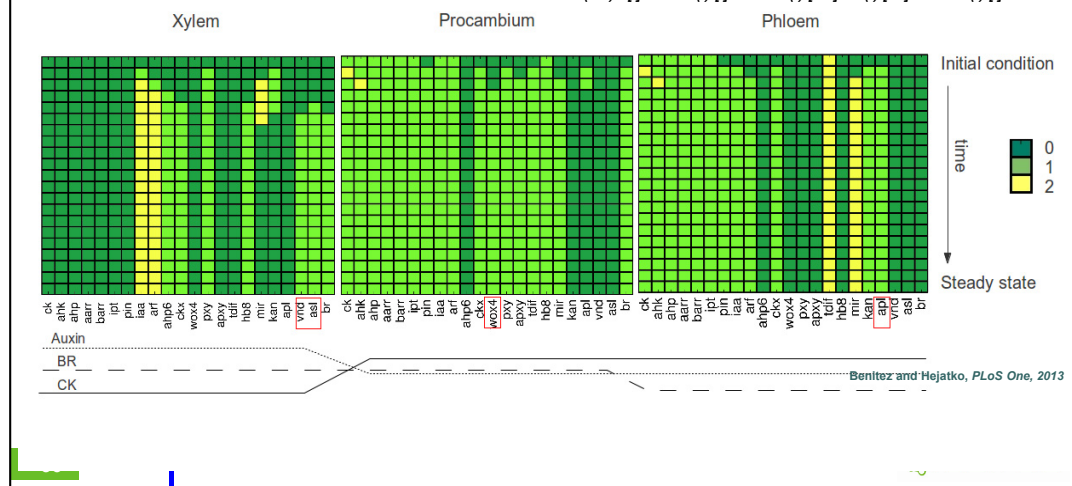
proportion of movable element

Modelování molekulárních regulačních sítí

- **Dobrý model** by měl být schopen **simulovat realitu**

$$\text{Static nodes: } g_n(t+1) = F_n(g_{n1}(t), g_{n2}(t), \dots, g_{nk}(t))$$

$$\text{Mobile nodes: } g(t+1)_{T[i]} = H(g(t)_{[i]} + D(g(t)_{[i+1]} + g(t)_{[i-1]} - N(g(t)_{[i]}) - b)$$



The initial conditions specify the initial state of some of the network elements (figure above) and are the following :

I) In the procambial position (central compartment), CK is initially available and there is an initial and sustained IAA input or self-upregulation. This condition is supported by several lines of evidence. Also *HB8*, a marker of early vascular development that has been found in preprocambial cells, is assumed to be initially present at this position. These conditions are not fixed, however. After the initial configuration, all the members of the CK and IAA signaling pathways, as well as *HB8*, can change their states according to the logical rules.

II) In the xylem and phloem positions, it is assumed that no element is initially active except for the CK signaling pathway and TDIF, both in the phloem position. The level of expression for a given node is represented by a discrete variable g and its value at a time $t+1$ depends on the state of other components of the network (g_1, g_2, \dots, g_N) at a previous time unit. The state of every gene g therefore changes according to:

$$g_n(t+1) = F_n(g_{n1}(t), g_{n2}(t), \dots, g_{nk}(t)) \quad (1).$$

In this equation, $g_{n1}, g_{n2}, \dots, g_{nk}$ are the regulators of gene g_n and F_n is a discrete function known as a logical rule (logical rules are grounded in available experimental data, for example see slide 20). Given the logical rules, it is possible to follow the dynamics of the network for any given initial configuration of the nodes expression state. One of the most important traits of dynamic models is the existence of steady states in which the entire network enters into a self-sustained configuration of the nodes state. It is thought that in developmental systems such self-sustained states correspond to particular cell types.

According to experimental evidence for the system under study, the hormone IAA, the peptide TDIF, and the microRNA MIR165/6 are able to move among the cells. In the case of TDIF and MIR165/6, the mobility is defined as diffusion and is given by the following equation:

$$g(t+1)_{T[i]} = H(g(t)_{[i]} + D(g(t)_{[i+1]} + g(t)_{[i-1]} - N(g(t)_{[i]}) - b) \quad (2),$$

where $g(t)_{T[i]}$ is the total amount of TDIF or MIR165 in cell (i). D is a parameter that determines the proportion of g that can move from any cell to neighboring ones and is correlated to the diffusion rate of g . b is a constant corresponding to a degradation term. H is a step function that converts the continuous values of g into a discrete variable that may attain values of 0, 1 or 2. N stands for the number of neighbors in each cell. Boundary conditions are zero-flux. In the case of IAA, the mobility is defined as active transport dependent on the radial localization of the PIN efflux transporters and is defined by the equation:

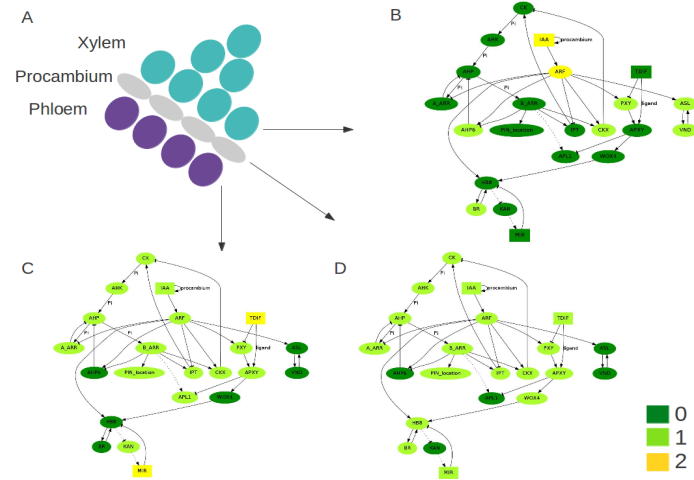
$$iaa(t+1)_{T[i]} = H(iaa(t)_{[i]} + Diaa(pin(t)_{[i+1]})(iaa(t)_{[i+1]}) + Diaa(pin(t)_{[i-1]})(iaa(t)_{[i-1]}) - N(Diaa)(pin(t)_{[i]})(iaa(t)_{[i]}) - b) \quad (3),$$

where $Diaa$ is a parameter that determines the proportion of IAA that can be transported among cells. The transport depends on the presence of IAA and PIN in the cells and b corresponds to a degradation term. As in equation 2, H is a step function that converts the continuous values to discrete ones and N stands for the number of neighbors in each cell. Boundary conditions for IAA motion are also zero-flux.

Using the logical rules, equations 1–3, and a broad range of parameter values (not shown here), it is possible fully to reproduce the results and analyses reported in the following sections (see the figure above for the simulation time course).

Modelování molekulárních regulačních sítí

□ **Dobrý model** by měl být schopen **simulovat realitu**



37

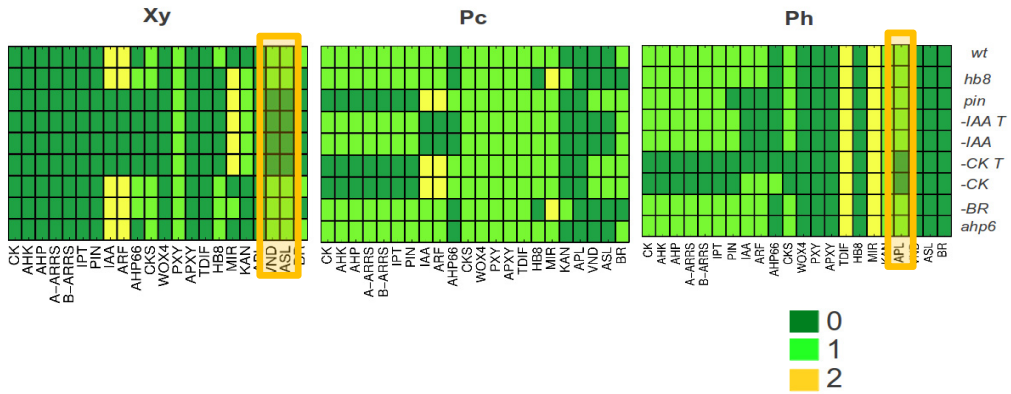
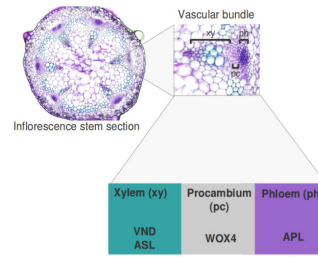
Benitez and Hejato, submitted

CEITEC

Another representation of the distinct expression profiles in the individual vascular bundle compartments (phloem, procambium and xylem).

Modelování molekulárních regulačních sítí

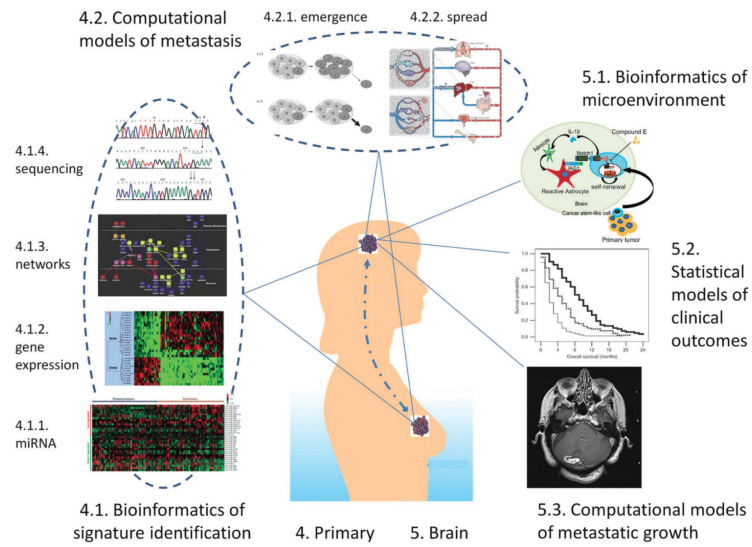
□ Simulace *mutantů*



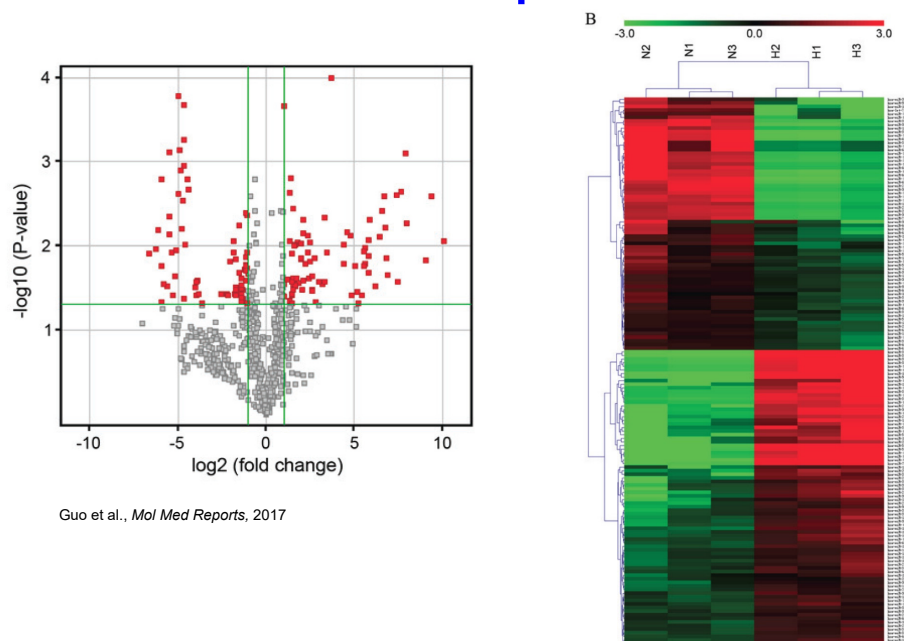
Osnova

- Definice Systémové biologie
- Nástroje
 - Genová ontologie
 - Bayesovské sítě
 - Modelování molekulárních/genových regulačních sítí
 - Odvození genových regulačních sítí z velkých omických datových sad

Systemová biologie ve výzkumu rakoviny



miRNA/mRNA profilování

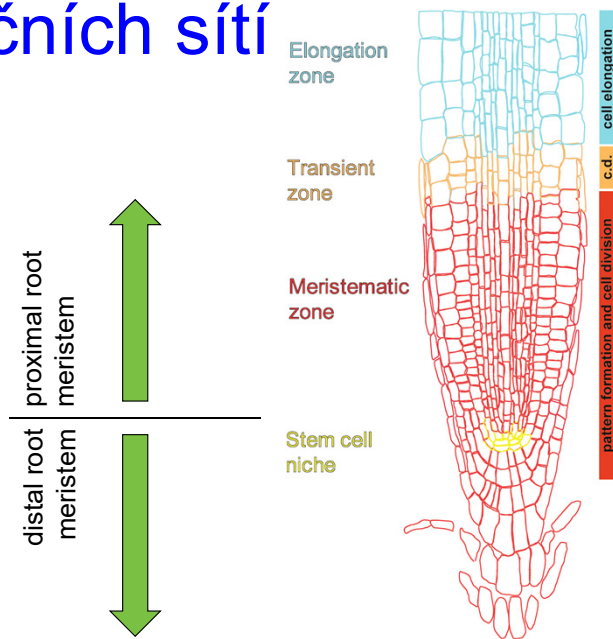


41

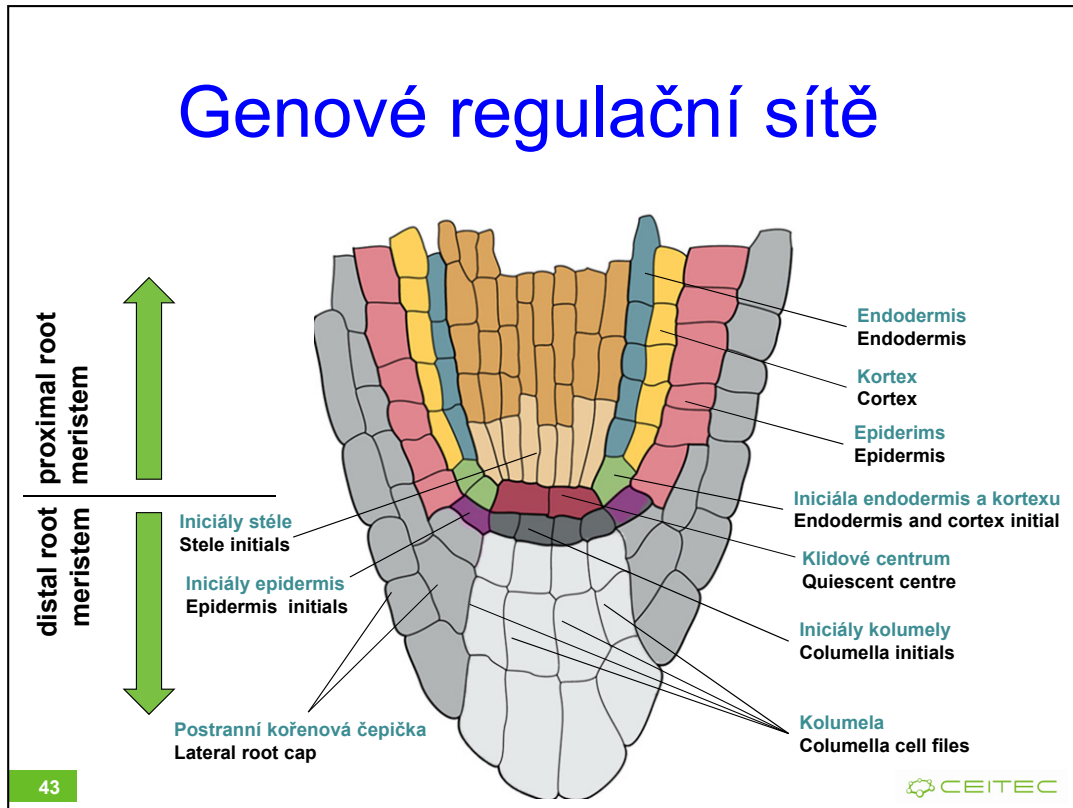
Hypertrophic scars (HS) are a fibroproliferative disorder of the skin, which causes aesthetic and functional impairment. However, the molecular pathogenesis of this disease remains largely unknown and currently no efficient treatment exists. MicroRNAs (miRNAs) are involved in a variety of pathophysiological processes, however the role of miRNAs in HS development remains unclear. To investigate the miRNA expression signature of HS, microarray analysis was performed and 152 miRNAs were observed to be differentially expressed in HS tissue compared with normal skin tissues. Of the miRNAs identified, miRNA-21 (miR-21) was significantly increased in HS tissues and hypertrophic scar fibroblasts (HSFBs) as determined by reverse transcription-quantitative polymerase chain reaction analysis. It was also observed that, when miR-21 in HSFBs was blocked through use of an antagomir, the phenotype of fibrotic fibroblasts *in vitro* was reversed, as demonstrated by growth inhibition, induction of apoptosis and suppressed expression of fibrosis-associated genes collagen type I α 1 chain (COL1A1), COL1A2 and fibronectin. Furthermore, miR-21 antagomir administration significantly reduced the severity of HS formation and decreased collagen deposition in a rabbit ear HS model. The total scar area and scar elevation index were calculated and were demonstrated to be significantly decreased in the treatment group compared with control rabbits. These results indicated that the miR-21 antagomir has a therapeutic effect on HS and suggests that targeting miRNAs may be a successful and novel therapeutic strategy in the treatment of fibrotic diseases that are difficult to treat with existing methods.

miRNA expression signature profiling in hypertrophic scars (HS). (A) Volcano plot presenting differentially expressed miRNAs between HS and paired (non-scar, obtained from donor sites during scar resection) NS tissue. miRNA microarray expression profiling from three paired HS and NS tissues was performed. Differentially expressed miRNAs were identified by fold change and a P-value calculated using Student's *t*-test. The threshold set to identify up and downregulated genes was a fold change ≥ 2 and $P < 0.05$. Red dots indicate points-of-interest that exhibit large-magnitude fold-changes (x-axis; log₂ of the fold change) and high statistical significance (y-axis: -log₁₀ of the P-value). (B) Hierarchical clustering showing differentially expressed miRNAs from HS samples compared with paired NS tissues. Each row represents one miRNA and each column represents one tissue sample. The relative miRNA expression is depicted according to the color scale. Red indicates upregulation and green indicates downregulation. N1-3 represents NS tissue samples, whereas H1-3 represents HS tissue samples. The differentially expressed miRNAs were clearly separated into clusters. miRNA, microRNA; hsa-miR, human microRNA; HS, hypertrophic scar; NS, normal skin.

Odvození genových regulačních sítí



Genové regulační síť

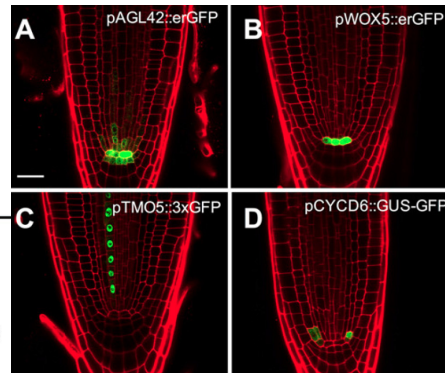


In the root, several functional and anatomical units could be recognized.

Along the longitudinal axis, the root meristem forms a distal root tip, including stem cell niche, columella and lateral root cap, proximal meristem with a population of rapidly dividing cells and elongation zone where cells leaving the root meristem undergo rapid elongation and mature.

Genové regulační sítě - GENIST

- Odvození GR sítí přes **GENIST**
 - **GE**ne regulatory **N**etwork **I**nference from **S**patio**T**emporal **d**ata algorithm
 - Kombinace **prostorových-časově-specifických profilů** **exprese genů**



44

Birnbaum et al., *Science*, 2003

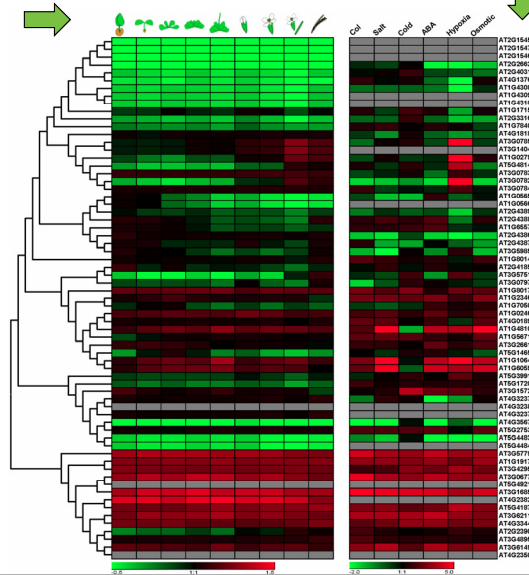
CEITEC

Specific subpopulations from the stem cell niche (SCN) were isolated via protoplasting the root (removing the cell wall enzymatically allowing to release the individual cells) of several specific reporter lines (A-D in the figure on the right) and GFP-positive cells were isolated using cell sorter. The mRNA was isolated and transcriptional profiling via NGS was performed.

By comparing the cell type-specific transcriptomes with developmental-specific root transcriptomes (isolating mRNA from meristematic (1, the figure on the left), elongation (2) and differentiation (3) zones), the stem cell-specific transcriptomes were identified.

Kombinace velkých omických datových sad

PLETIVO/ČAS



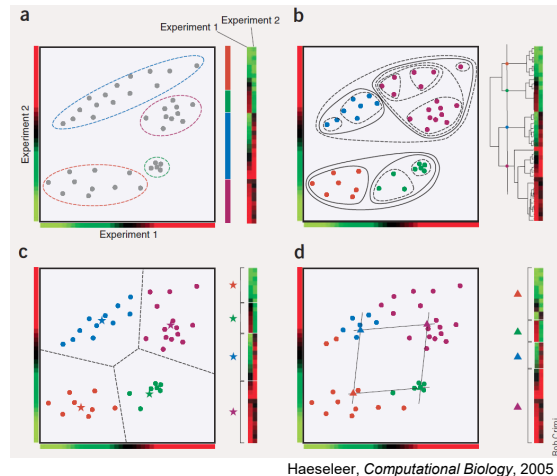
GENY



AT2G16460
AT2G16470
AT2G16480
AT2G26620
AT2G40310
AT4G13740
AT1G62080
AT1G62090
AT1G17180
AT2G23160
AT1G78400
AT4G18180
AT3G07880
AT2G16490
AT1G02790
AT5G4140
AT3G07830
AT3G07820
AT3G07840
AT1G08860
AT2G43890
AT1G08870
AT1G08880
AT2G43870
AT1G08890
AT1G08910
AT1G08920
AT3G57610
AT1G08910
AT1G08920
AT1G08930
AT1G08940
AT1G08950
AT1G08960
AT1G08970
AT1G08980
AT1G08990
AT1G09000
AT1G09010
AT1G09020
AT1G09030
AT1G09040
AT1G09050
AT1G09060
AT1G09070
AT1G09080
AT1G09090
AT1G09100
AT1G09110
AT1G09120
AT1G09130
AT1G09140
AT1G09150
AT1G09160
AT1G09170
AT1G09180
AT1G09190
AT1G09200
AT1G09210
AT1G09220
AT1G09230
AT1G09240
AT1G09250
AT1G09260
AT1G09270
AT1G09280
AT1G09290
AT1G09300
AT1G09310
AT1G09320
AT1G09330
AT1G09340
AT1G09350
AT1G09360
AT1G09370
AT1G09380
AT1G09390
AT1G09400
AT1G09410
AT1G09420
AT1G09430
AT1G09440
AT1G09450
AT1G09460
AT1G09470
AT1G09480
AT1G09490
AT1G09500

Genové regulační sítě - GENIST

- Odvození GR sítí přes **GENIST**
 - **shlukování (klastrování) genů**
 - Expresní podobnost za různých podmínek/genetické pozadí, časové body, ...
 - **Odvození spojení uvnitř klastru**
 - **Selekce** potenciálních **regulátorů** a **ko-regulátorů**
 - Na základě **časové korelace** ve změně **exprese** a/nebo **specifikace uživatele**
 - **Modelování dynamické Bayesovské sítě**



46

CEITEC

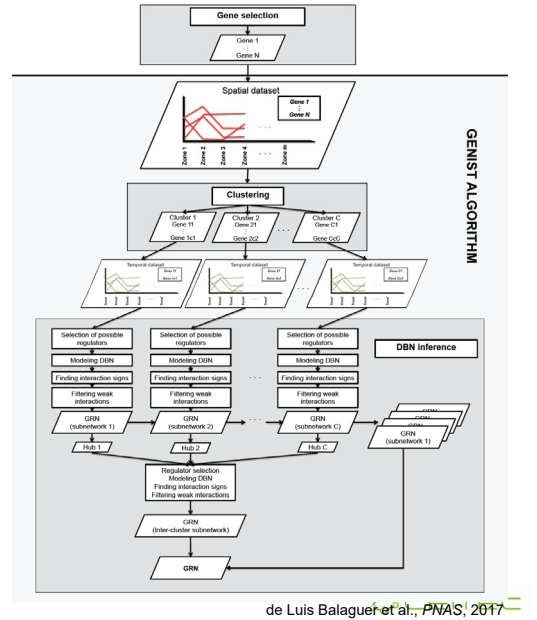
GENIST algorithm

The MATLAB source code for GENIST is publicly available at <https://github.com/madeluis/GENIST>.

For the detailed description of the procedure, see de Luis Balaguer et al., 2017, SI (<https://www.pnas.org/content/114/36/E7632/tab-figures-data>)

Genové regulační sítě - GENIST

- Odvození GR sítí přes **GENIST**
 - **shlukování (klastrování) genů**
 - Expresní podobnost za různých podmínek/genetické pozadí, časové body, ...
 - **Odvození spojení uvnitř klastru**
 - **Selekce** potencionálních **regulátorů** a **ko-regulátorů**
 - Na základě **časové korelace** ve změně **exprese** a/nebo **specifikace uživatele**
 - **Modelování dynamické Bayesovské sítě**



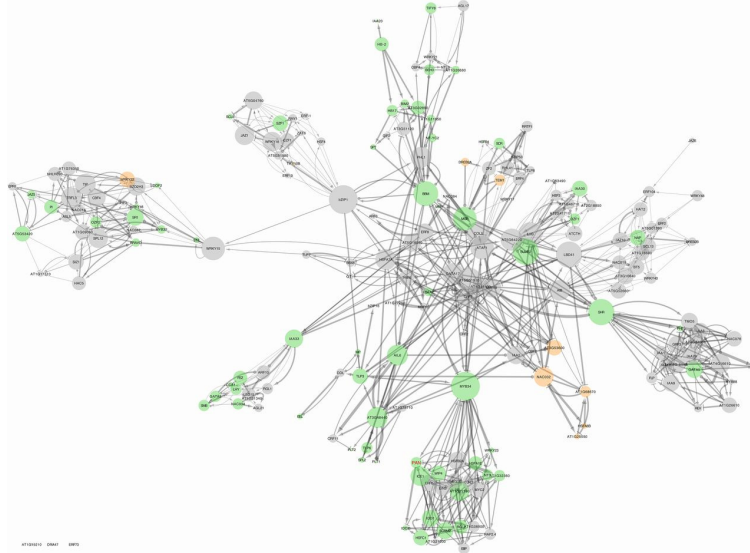
GENIST algorithm

The MATLAB source code for GENIST is publically available at <https://github.com/madeluis/GENIST>.


For the detailed description of the procedure, see de Luis Balaguer et al., 2017, SI (<https://www.pnas.org/content/114/36/E7632/tab-figures-data>)

GENIST block diagram. GENIST is implemented in MATLAB, and is composed of two consecutive steps, clustering and GRN inference. Clustering is performed based on a spatial dataset. Each resulting cluster is independently processed by the GRN inference step, based on a temporal dataset.

Genové regulační sítě - GENIST

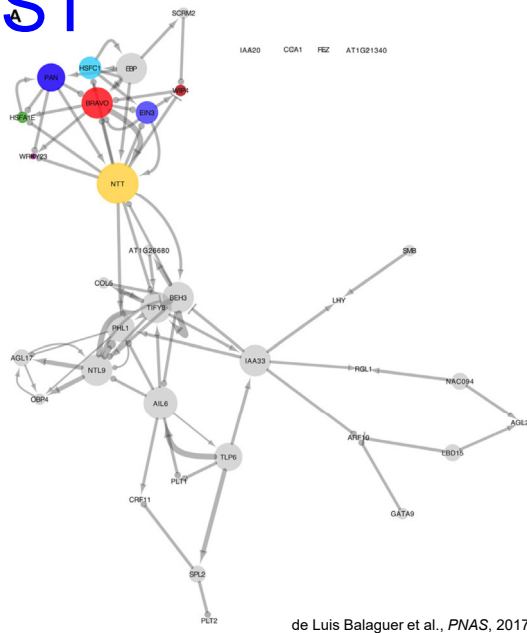


48


de Luis Balaguer et al., *PNAS*, 2017. 

Network of the 201 TFs enriched in the SCN, inferred with the 12 developmental time points of the *Arabidopsis* root. Clusters of nodes indicate groups of TFs functionally related or functioning in the same cell type. Node sizes indicate importance of the nodes in terms of the number of TFs that they regulate. The highly connected groups of genes or subnetworks correspond to the dynamic Bayesian network (DBN) inferred for each cluster. Green (orange) nodes represent factors that are differentially down-regulated (up-regulated) in the pan mutant with respect to Col-0 wild type. Blue represents the PAN node.

Genové regulační sítě - GENIST

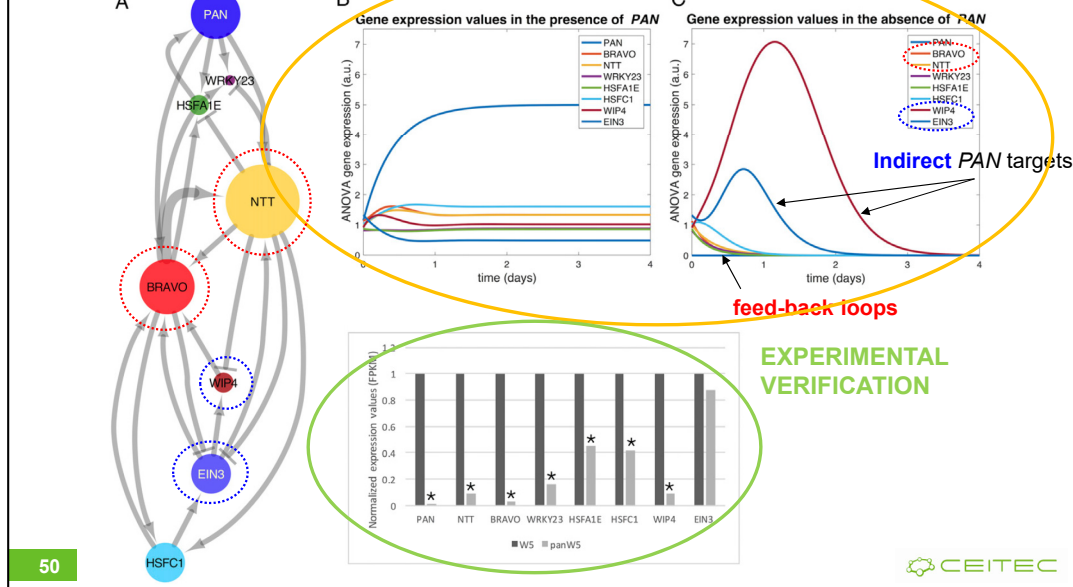


49

de Luis Balaguer et al., *PNAS*, 2017 

Network of QC-enriched TFs. (A) Network among the QC-enriched TFs inferred with the 12 developmental time points of the Arabidopsis root. Node sizes indicate importance of the nodes in terms of the number of TFs that they regulate. Color-coded nodes represent genes downstream of PERIANTHA (PAN) that were used for the mathematical model and experimental confirmations.

Genové regulační síť - GENIST



PAN subnetwork in the QC inferred with the 12 developmental time points of the Arabidopsis root. (A) Optimal configuration (combination of signs— activation or repression—of the regulations that were inferred with undefined signs, which best fits the data in the simulations of the equations) of the subnetwork of PAN and its downstream targets. (B and C) Resulting expression values of PAN and its downstream targets, over time, after simulating the optimal configuration of the model. Simulations were run for 5 d and plots are shown until all factors reached steady states in the WT and pan mutant simulations. (B) Model simulated with the fitted equation parameters. (C) Model simulated with the PAN-associated parameters set to zero to simulate a pan mutant situation. (D) Normalized expression values of PAN and its predicted downstream targets in Col-0 wild type and in pan mutant. Statistically significant changes of expression between the mutant and the wild type, * $q < 0.05$.

In the WT simulation, all targets reached steady states by day 1 with subtle changes of expression during the transients (time length until expression values reach their steady states). On the contrary, the pan mutant simulation showed that EIN3 and WIP4 presented high expression values during the transients and reached steady states at later stages (days 3 and 4, respectively). These delayed responses and initial activations of EIN3 and WIP4 reflect the prediction that these genes are indirectly affected by PAN. Further, the dynamics of our simulations depict that BRAVO, NTT, and WIP4 are, in our equations, connected through feedback loops. During the transient phase of the mutant simulation, NTT and BRAVO show an exponential decay, which is consistent with the prediction that they activate each other in the absence of PAN. However, their steady states are not immediately reached since they are activated by WIP4 and EIN3. Conversely, WIP4, which is repressed by a decaying NTT, shows high levels of expression.

With the exception of indirect target EIN3, the qRT PCR-based gene expression quantification confirmed the predicted expression values.

Klíčové koncepty

- Systémová biologie se pokouší identifikovat nové vlastnosti/chování skupin funkčních podjednotek (regulátorů/molekul), které nejsou prostým součtem vlastností jednotlivých podjednotek, ale jsou novou vlastností závislou na způsobu jejich vzájemné interakce
- Využívá matematické modely, často Bayesovské sítě
- Genové regulační sítě lze identifikovat i pomocí (semi)automatických nástrojů z velkých datových sad (např. genové exprese na úrovni celého genomu)
- Využití metod strojového učení („umělá inteligence“)

Diskuse